International Journal of Nanoelectronics and Materials
IJNeaM
ISSN 1985-5761 | E-ISSN 2232-1535

Preparation and Study Ag Nanoparticles via PLAL Technique: Influence of Different Number of Pulses

Thuraya Yarb Sabri 1[a], Saif Khalel Jasim 2[b,c]*, Ammar Ayesh Habeeb 3[d] and Awatif Saber Jasim 4[a]

[a] Department of Physics, College of Science, University of Tikrit, Tikrit Iraq
[b] Ministry of Education. Diyala Education Directorate , Diyala, Iraq
[c] Department of Radiology Techniques, Bilad Alrafidain University College, Diyala, 32001, Iraq
[d] Department of Physics, College of Science, University of Diyala, Diyala, Iraq
Corresponding author. Tel.: +0-000-000-0000; fax: +0-000-000-0000; e-mail: Saifalaosy@gmail.com [2,3]

Received 11 January 2023, Revised 12 June 2023, Accepted 13 July 2023

ABSTRACT

Using a quick, easy, and effective one-step synthesis method called Q-switched neodymium-doped yttrium aluminum garnet (Nd:YAG)-pulsed laser ablation in liquid (PLAL), silver nanoparticles (NPs) are physically created. By using a pulsed laser at 532 nm to vaporize a metallic target (in this case, silver) submerged in deionized water, silver colloidal solutions are separately created. Laser parameters pulse of number (100, 200, and 300 pulse/sec) with constant ablation energy 500 mJ. The cubic crystalline structure of Ag particles was revealed by XRD, along with the formation of a pure cubic crystal structure of Ag particles and another cubic crystal structure attributed to AgO particles. The subsequent FESEM images showed the formation of highly spherical crystals (mean diameter 25.003 nm, 24.43 nm, and 9.75 nm). UV-Vis analysis reveals the absorption band of Ag NPs at (407, 406, and 404 nm), and the energy gap was (2.74, 2,79, and 2.95 eV) respectively. *The diagnosis of spherical colloidal Ag-NPs was approved by FESEM, and the PL spectra show two peaks at 320 and 639 nm, confirming the purity of the produced Ag-NPs. It is clear that the possibility of using the prepared nanoparticle in optoelectronics applications such as optical detectors, solar cells, and optical sensors.*

Keywords: Silver, Laser, Ablation, Nanoparticles, Pulse, and Liquid.

1. INTRODUCTION

Nanotechnology has become in different disciplines so that experts in one field can comprehend advancements in another. Chemical reduction, microwave-aided procedures, radiation chemical reductions, and other technologies are all used in the creation of nanoparticles [1]. Application biosensors, photocatalysis, nanomedicine, [2,3] cosmetics, and other items have all made use of these nanostructures. Many ways have been used to synthesize nanoparticles of inorganic metals (such as Au, Ag, and others) and semiconductors over the years (Zno, Ge, GaAs, Si, etc.) [4,5]. To make NPs, bulk material is employed in a physical approach that involves the condensation of a gaseous component. In this connection, the pulse laser ablation (PLAL) approach is an important physical method for producing nanostructures that has been demonstrated to be reliable and versatile [6]. Furthermore, more research needs to be done on the shape, structure, and media sensitivity of uniform and well-dispersed NPs produced inside of liquid suspension [7]. Due to its simplicity, cost-effectiveness, and speed in reactive quenching of ablated species at room temperature, the (PLAL) technology has recently been acknowledged as a promising nanofabrication pathway [8].

The interaction of generated plasma with liquid medium, which is distinctive surface chemistry, repeatability on a large scale, high purity, and stability Colloids can be handled easily, and NPs, particularly metal-NPs, can be produced quickly [9]. Meanwhile, it is a versatile and environmentally safe method that permits the creation of a wide range of nanostructures without the use of harmful chemicals. The shape of NPs generated by the PLAL process can be improved by altering the laser parameters (wavelength, fluence, pulse width, and repetition rate) as well as the solvent type [10,11].

2. MATERIAL AND METHODS

High purity (above 96%) was purchased from a metal and chemical store in Baghdad, Iraq, silver plate with dimensions of 15 mm x 15 mm x 2 mm was employed as the target substance. To remove all surface impurities, the sliver target was cleaned with ethanol and washed with distilled water. Figure 1. depicts the PLAL process experiment setup. Nanosecond laser pulses were used to ablate an Ag target, resulting in slimy AgNPs in deionized water. A Q-switched Nd:YAG laser beam (532 nm wavelength, pulse duration of 10 ns, and repetition rate of 1 Hz) with ablation energy constant 500 mJ and pulses number different (100, 200, and 300 pulse/sec).

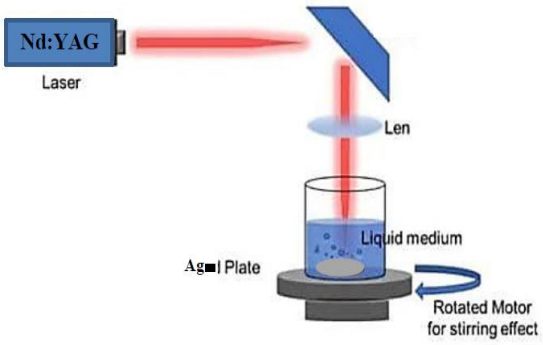

Figure 1. Schematics of PLAL set-up for the synthesis of AgNPs in liquid.

2. Methods

After we prepared the silver nanoparticles at room temperature, we used the well-known distillation drop-casting method to prepare a membrane of silver nanoparticles to measure its XRD using a model of Bruker D2 Phase diffract meter, the scanning range was 10° to 90° for 2Θ it was drawn using the Origin Lab 2018 program. AgNP ore morphology was studied using the field emission scanning electron microscope (FESEM) the size of the particle diameters was calculated using the (Image j) program, and then a statistical drawing was made for it using the Origin Lab 2018 program, whale Uv-Vis, FTIR, and PL measurement they were plotted and analyzed using the origin lab 2018 program.

2. 3. RESULTS AND DISCUSSION

Figure 2 shows X-ray diffraction patterns which were obtained and analyzed for AgNPs prepared with an optimum laser ablation sample at (300 pulse/sec). The crystallite size was calculated by applying Scherrer's equation to the full-width half maximum (FWHM) and Miller indices. The silver particles have formed a pristine cubic crystal structure, as shown by the X-ray diffraction patterns, which are similar to the standard patterns (JCPDS 89-3722), lattice parameters, and angles (a = b = c = 4.0855), and (α = β = γ =90°), respectively. Additionally, they demonstrate the development of a second cubic crystal structure, which is attributed to AgO particles, with the same standard patterns (JCPDS 03-5662), lattice parameters, and angles (a = b = c = 4.8160), and at a rate of (300) pulses per second. We notice four peaks, which correspond to the orientations (111), (200), (220), and (311) correspondingly, at angles of 38.35, 44.5, 64.8, and 77.65 as in Table (1). Additionally, we noticed one peak at an angle of 38.35°, which is consistent with the orientations (111) associated with AgO particle orientations [12]. No film was obtained for the samples that were prepared using the number of pulses 100 and 200 pulse/sec, due to the low concentration of the prepared materials due to the small number of pulses.

Table 1. Experimental and standard results of X-ray diffraction of AgNPs nanoparticles

2Θ (deg) Practical	2Θ (deg) Standard	FWHM (deg)	crystalline size "D" (nm)	d_{hkl} (A°) Practical	d_{hkl} (A°) Standard	(hkl)	$h^2+k^2+l^2$
38.35	38.078	0.1125	74.79	2.34	2.36	(111)	3
44.5	44.256	0.293	29.31	2.032	2.0450	(200)	4
64.8	64.376	0.2047	45.98	1.437	1.4460	(220)	8
77.65	77.312	0.6126	10.12	1.2327	1.2331	(311)	11

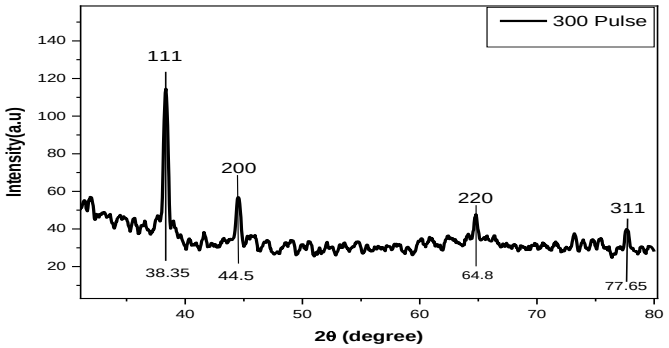

Figure 2. *X-ray diffraction patterns of silver nanoparticles using numbers of pulses* (300 pulse /sec).

3.2 FESEM Results

Figure 3 shows the FESEM pictures of AgNPs synthesized in liquid medium by 532 nm laser pounding. It is apparent that the variability of parameter laser Nd-YAG role plays a significant cycle in the size and type of the expansion morphology of AgNPs sample Ag us in different number of pulses (100, 200, and 300 pulse/sec). Obtained on the average diameter is (25.003 nm with a standard deviation of 10.987 nm) and size distribution (ranging from 5.44 nm to 45.47 nm), the average diameters (24.431 nm with standard deviation of 8.251 nm) and size distribution (ranging from 4.33 nm to 56 nm), the average diameters (9.75 nm with standard deviation of 4.251 nm) and size distribution (ranging from 4.7 nm to 18.68) respectively. If the number of pulses increases, a smaller average diameter, as shown in Table 2.

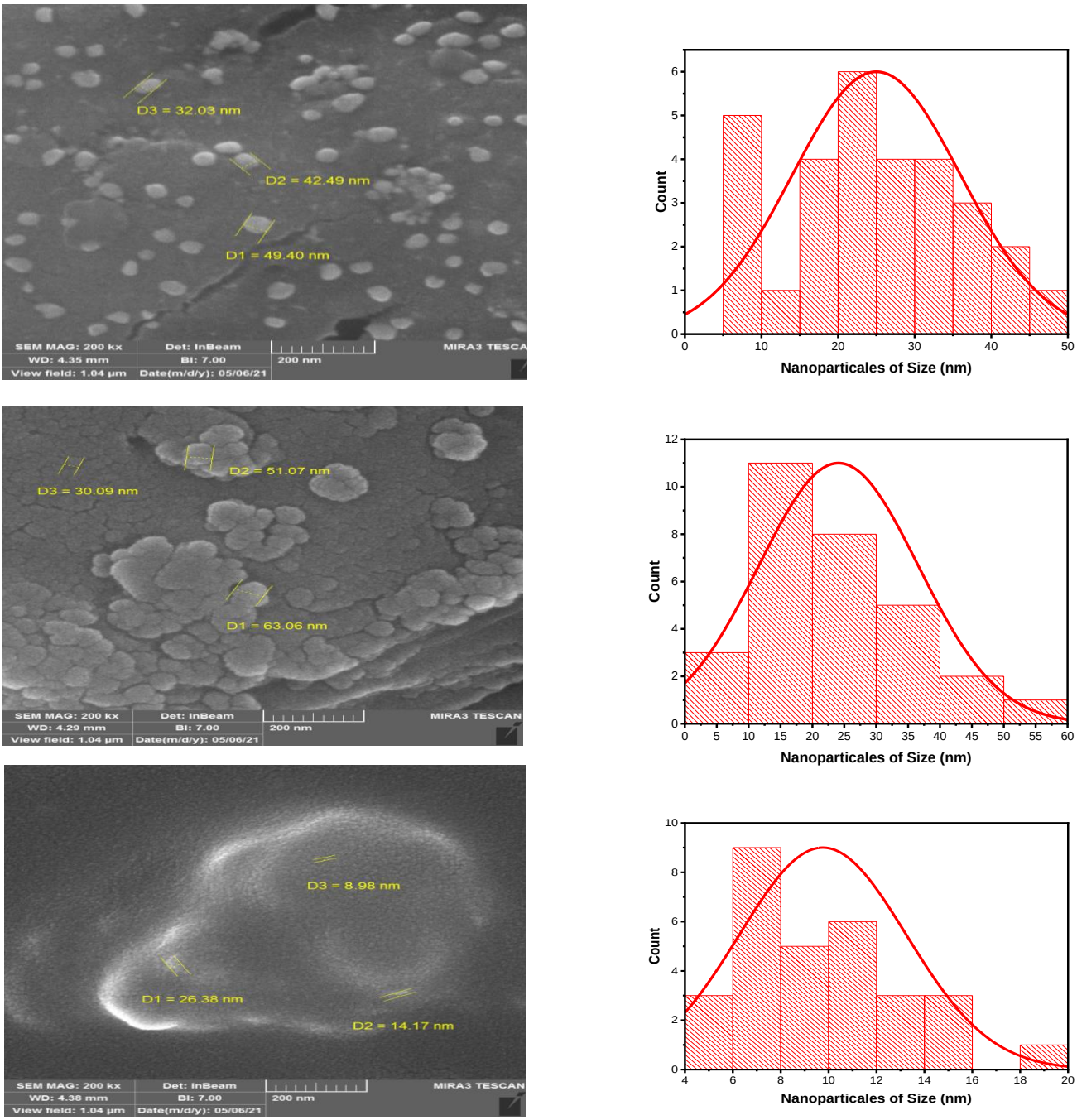

Figure 3. FESEM micrograph images of AgNPs at (100,200, and 300) pulses/sec, with *size distributions*.

Table 2. FESEM results for AgNPs by changing the number of pulses.

Sample (Pulse/sec)	Average particle size (nm)	Standard deviation (nm)
100	25.003	10.987
200	24.431	8.251
300	9.75	4.251

3.3 Optical results

Figure 4 shows Uv-Vis spectro which has been obtained by laser ablation of silver (Ag) bulk target in a different number of pulses (100, 200, and 300 pulse/sec) respectively. It is demonstrated that the nanoparticle's transmittance and ultraviolet-visible optical absorption spectra are the result of the colloid products. A deeper color indicates a higher level of nanoparticle concentration. It has been demonstrated that the surface plasmon resonance (SPR) absorption peak's position and width are sensitive to the intensity and repetition rate of the laser pulses used for ablation. Furthermore, as the number of pulses grew from 100 to 300 pulse/sec the intensity of the SPR absorption peak was increased. Insets (2) in Figure 4 shows color change in relation to the number of pulses. AgNPs' high quantum confinement was said to be responsible for the increase in absorption peak intensity and concomitant peck shift, which is supported by a FESEM image. The quantum size confinement effect might lead to a change in the absorption peak in smaller AgNPs by raising the energy needed for the ground state and excited state transitions [13,14]. The strength of the SPR absorption peak was increased, and the peak position showed a shift between 407, 406, and 404 nm respectively, as shown in Insets(1). The absorbance of AgNPs increases with the number of laser pulses (1.13, 0.77, and 0.77 a.u) respectively.

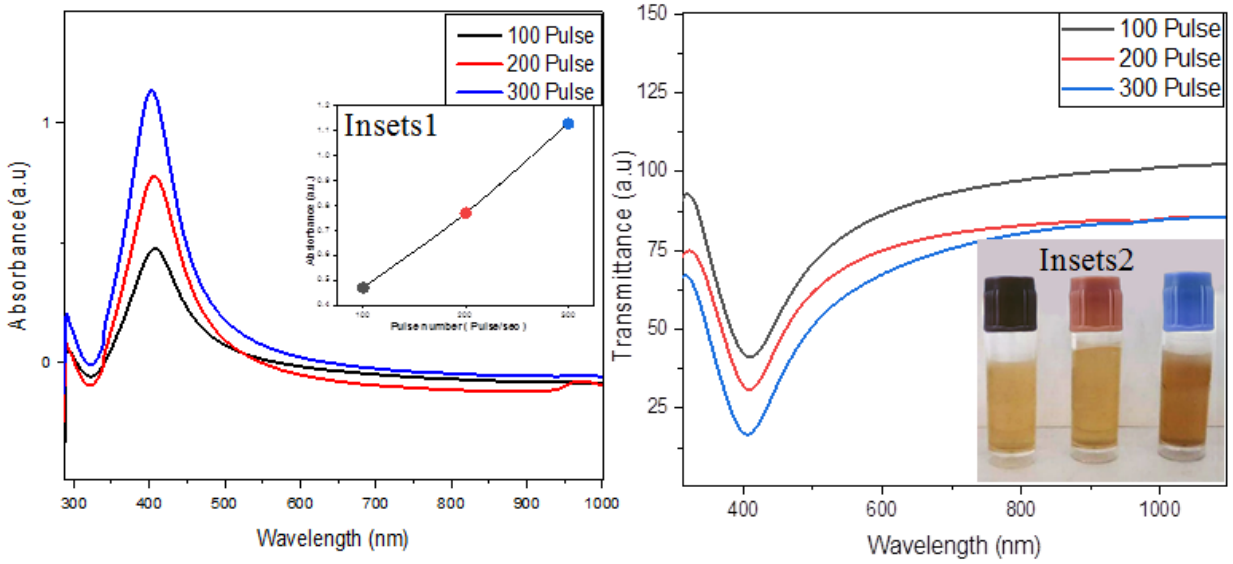

Figure 4. UV-Vis spectra absorption and transmittance of AgNPs at pulses of numbers. Inset (1) Absorbance as a function of the pulses of number, Inset (2) Color change in relation to the number of pulses.

Figure 5. Energy gap (Eg) in is the band-gap energy, which can be computed using the equation Eg = 1240/g (eV), where g is the absorption edge determined by the intersection of the absorption curve's tangent and the abscissa coordinate. [15] For the sample prepared at 100 pulses, the energy gap had a value of 2.95 eV, while for the sample prepared with 200 pulses, the energy gap had a value of 2.79 eV, and the energy gap of 2.74 eV was for the sample prepared with 300 pulses. A higher energy gap was obtained for the sample with the most number of pulses and the lowest energy gap for the sample with the least number of pulses and their values are explained in Table 3.

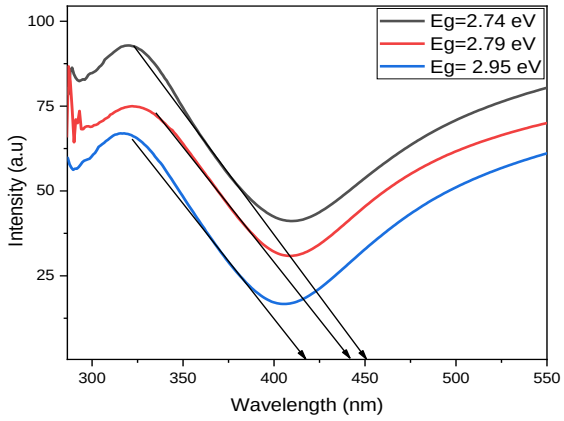

Figure 5. Energy gap of Ag NPs at different pulse of number.

Figure 6 shows PL spectra of AgNPs, at room temperature. It shows PL emission spectra of assynthesized AgNP grown in solution media at excitation wavelength of 300 nm as a function of wavelength. Over excitement of the AgNPs by accident laser photon the electrons were uploaded to the edgy states toward the optical band gap. The spectrum of a solution containing oxide particles AgNPs shows two peaks, the first in the ultraviolet region at (320-321 nm), called emission near the edge of the beam and the top, the second is in the visible region as in Inset (1). The reason for the resurgence of the first summit is the reunification electrons with holes that are emitted while the second peak is emitted at 639 nm (Inset (2)) due to the presence of surface defects. From the luminescence spectrum, we find the energy gap value because when some electrons move from the valence band to the conduction band, they emit photons corresponding to the energy gap of the NP. It is also noted that the size of the NP decreases with the increase in the number of pulses which is accompanied by a decrease in the particle size for NP [16].

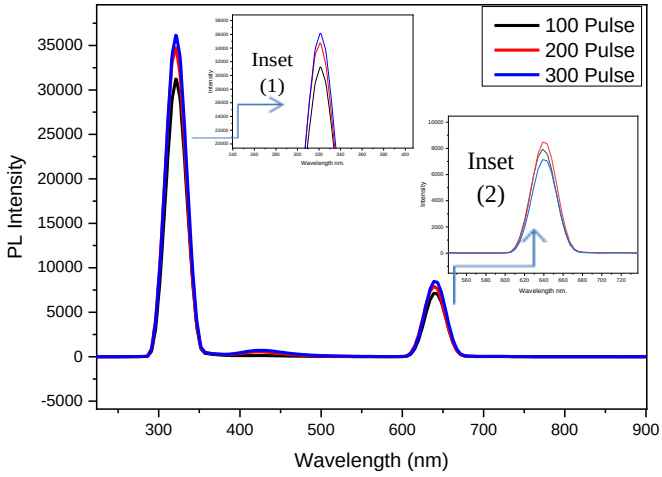

Figure 6. PL spectra of AgNPs at different pulses of numbers.

Table 3. Various features of AgNPs optical at different pulses of numbers

AgNPs Pulses number (pulse/s)	SPR (nm)	Eg (eV)	PL Peak shift1(nm)	PL Peak shift2(nm)
100	407	2.95	320	639
200	406	2.79	320	639
300	405	2.74	321	369

According to Mafuné et al.[16] the most typical liquid medium for the production of metal nanoparticles is water. The use of water as a synthesis medium raises the possibility of producing a large number of oxide or hydroxide species due to interactions between the target material and dissolved oxygen or oxidizing reactions sparked by the plasma-induced breakdown of water. Figure 7 shows FTIR spectra species (such as hydroxyl groups) which can adsorb on the NP surface, creating highly charged surfaces that aid in the electrostatic stabilization of the synthesized nanoparticles. Because it is cheap, secure, has a high heat capacity, and does not absorb laser light, water is a common ablation medium. A variety of samples, each of which contained numerous distinct vibration bands

The spectra clearly demonstrated the presence of several chemical functional groups connected to active molecular bonds attached to various samples, which consisted of multiple unique vibration bands. The presence of several chemical species was amply demonstrated by the spectra. functional groups connected to molecules via active bonds. shows the FTIR spectra of different samples, which featured multiple distinctive vibration bands. The existence of numerous chemical species functional groups linked to the active molecular bonds was clearly seen in the spectra [16,17,18]. The vibration of the OH (hydroxyl group) and hydrogen stretching bonds in water molecules, respectively, were assigned to the IR bands at 3314 cm^{1} [18]. Overtones were approved for the band at 2100 cm^{1}. O–H–O scissoring bending is assigned to the bands around 1637 cm^{1}.

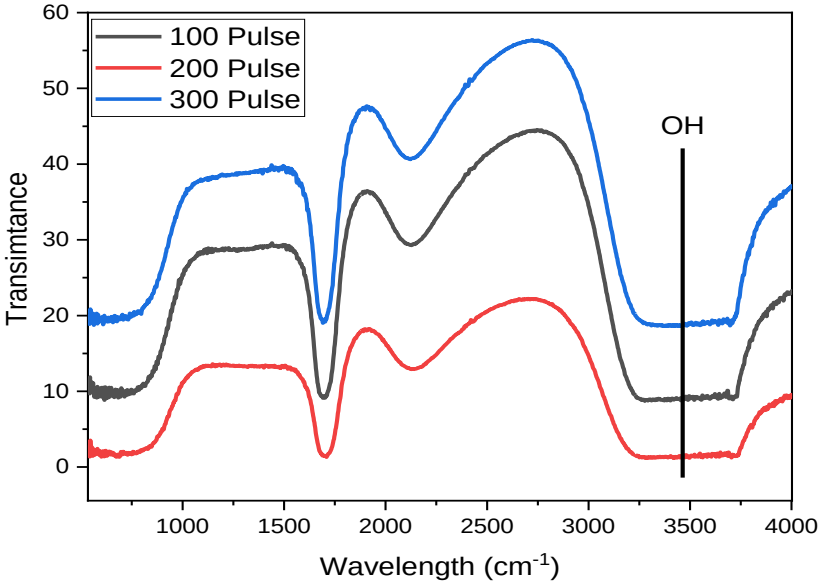

Figure 7. FTIR spectra of AgNPs at pulses of numbers.

4. CONCLUSION

The technique is anticipated to provide a basis for the creation of AgNPs with the superior optical properties, desired shape, tunable structure, and long-term stability required for a number of applications. With the possibility of controlling the laser parameters such as changing the number of pulses and constant the ablation energy frequency values. Highly spherical colloidal AgNPs were synthesized in deionized water deionized water using the pulse laser ablation in liquid technique with various laser pulses. For the characterization of synthesized NPs in liquid, various spectroscopy analytical equipment, such as UV-Vis, PL, and FTIR analysis, was used. The effect of different PLAL on morphology, optical properties, size, and bonding structure via Xrd and FESEM. The remarkable characteristics of the results suggest that the development of biophotonic and biomedical technologies could benefit from the use of Ag nanocolloids with good optical characteristics generated in a liquid medium.

ACKNOWLEDGEMENTS

The authors would like to thank the College of Science for agreeing to work in the college laboratories.

REFERENCES

[1] S. Jayachadran, D. Khetan, K. Pestonjamasp, et al., "A Review on Biological Building Blocks and its Applications in Nanotechnology," *IOP Conference Series: Materials Science and Engineering*, vol. 810, no. 1, IOP Publishing, 2020.

[2] E. Botzung-Appert, et al., "Polyaromatic luminescent nanocrystals for chemical and biological sensors," *Chemistry of Materials*, vol. 16, no. 9, pp. 1609-1611, 2004.

[3] T. D. Tran, T. H. Nguyen, and T. B. Nguyen, "Silver nanostructure on ablated silicon wafer prepared via pulsed laser ablation for surface enhanced Raman spectroscopy," *Journal of Raman Spectroscopy*, 2022.

[4] N. Nedyalkov, et al., "Tuning optical properties of noble metal nanoparticle-composed glasses by laser radiation," *Applied Surface Science*, vol. 463, pp. 968-975, 2019.

[5] M. Xie, et al., "Nano-curcumin prepared via supercritical: Improved anti-bacterial, anti-oxidant and anti-cancer efficacy," *International Journal of Pharmaceutics*, vol. 496, no. 2, pp. 732-740, 2015.

[6] A. Hahn, S. Barcikowski, and B. N. Chichkov, "Influences on nanoparticle production during pulsed laser ablation," *Pulse*, vol. 40, no. 45, p. 50, 2008.

[7] M. Alhajj, et al., "Customization of structure, morphology and optical characteristics of silver and copper nanoparticles: Role of laser fluence tuning," *Applied Surface Science*, 2022.

[8] G. Kumar, E. P. Shuaib, and D. Sastikumar, "Photoluminescence properties of carbon nanoparticles synthesized from activated carbon powder (4% ash) by laser ablation in solution," *Materials Research Bulletin*, vol. 91, pp. 220-226, 2017.

[9] H. Imam, et al., "Effect of experimental parameters on the fabrication of gold nanoparticles via laser ablation," 2012.

[10] A. S. Jasim, S. K. Jasim, and A. A. Habeeb, "Synthesis of Cinnamon Nanoparticles by Using Laser Ablation Technique," *Iraqi Journal of Physics (IJP)*, vol. 19, no. 49, pp. 7-14, 2021.

[11] I. X. Yin, J. Zhang, I. S. Zhao, M. L. Mei, Q. Li, and C. H. Chu, "The Antibacterial Mechanism of Silver Nanoparticles and Its Application in Dentistry," *International Journal of*

Nanomedicine, vol. 15, pp. 2555-2562, Apr. 2020.

[12] A. A. Kamil, N. A. Bakr, T. H. Mubarak, and J. Al-Zanganawee, "Synthesis and study of the optical and structural properties of Au and Ag nanoparticles by pulsed laser ablation (PLAL) technique," *Digest Journal of Nanomaterials & Biostructures (DJNB)*, vol. 16, no. 4, 2021.

[13] P. Slepička, et al., "Methods of gold and silver nanoparticles preparation," *Materials*, vol. 13, no. 1, 2019.

[14] A. A. Salim, et al., "Pulse laser ablated growth of Au-Ag nanocolloids: Basic insight on physiochemical attributes," *Journal of Physics: Conference Series*, vol. 1484, no. 1, IOP Publishing, 2020.

[15] S. N. Rashid, et al., "Synthesized Zinc Nanoparticles via Pulsed Laser Ablation: Characterization and Antibacterial Activity," *Karbala International Journal of Modern Science*, vol. 8, no. 3, pp. 462-476, 2022.

[16] R. A. Ismail, et al., "Preparation and characterization of colloidal ZnO nanoparticles using nanosecond laser ablation in water," *Applied Nanoscience*, vol. 1, no. 1, pp. 45-49, 2011.

[17] H. Muto, et al., "Estimation of surface oxide on surfactant-free gold nanoparticles laser-ablated in water," *The Journal of Physical Chemistry C*, vol. 111, no. 46, pp. 17221-17226, 2007.

[18] S. K. Jasim, A. S. Jasim, and A. A. Habeeb, "Growth Cinnamon Nanoparticles in Different Liquid by Pulsed Laser Ablation in Liquid PLAL," *MJPS*, vol. 8, no. 2, 2021.